INVESTIGATION OF CLOSE-TO-WALL WIRELESS SENSOR DEPLOYMENT USING 2D FINITE-DIFFERENCE TIME-DOMAIN MODELLING

Y. Wu and I. J. Wassell

Computer Laboratory, University of Cambridge, Cambridge, CB3 0FD, United Kingdom
yw264@cam.ac.uk, ijw24@cam.ac.uk

ABSTRACT

When Wireless Sensor Networks (WSNs) are deployed in a railway tunnel environment, the available deployment positions and equipment size are restricted by regulations from the infrastructure owners in order to maintain the loading gauge. As we have discovered in the Aldwych tunnel [1], antennas mounted near to the tunnel wall worsens the path loss (PL) performance at 868MHz and 2.45GHz. However, no literature exists concerning the detailed effects of close to wall antenna mounting and its impact on wireless sensor deployment. Currently, 2.4GHz is the preferred operating frequency, since it is employed by many of the existing commercially available low power wireless communication systems. In this paper, the Finite-Difference Time-Domain (FDTD) method [2] has been used to analytically explore the radiation patterns (RPs) of a 2.4GHz antenna mounted at different distances away from a tunnel wall constructed from different materials, i.e., cast iron, concrete and polythene.

1. INTRODUCTION

Changes in geometry, stress state and material deterioration are the major causes of damage in tunnels. In general, the damage is difficult to assess through conventional methods. Consequently, there has been a lot of recent work in the field regarding the use of Wireless Sensor Networks (WSNs) for this purpose. WSNs are becoming an increasingly common tool for monitoring and assessing the condition of aged civil infrastructure. The benefits of WSNs over wired networks include the ease of deployment and lower costs due to lack of wiring. However, in practice, the process of deploying WSNs presents a new set of challenges, such as choices of sensor nodes, power harvesting, network topology and its optimisation, data mining, security, radio propagation and development of common communication protocols for different systems as each deployment is strongly dependent on the individual application. These matters are further complicated by a lack of standards and a wide range of different wireless networking hardware and protocols. In addition, little is known about the radio propagation in particular environments. For example in a tunnel, factors such as transmit frequency, antenna position, tunnel diameter, building material and course [3-7] can in various ways affect the radio propagation. Even so, there are still many other factors, which need to be addressed. Here we present our investigation concerning wireless sensor deployment for a close-to-wall scenario using the finite-different time-domain (FDTD) technique.

The FDTD technique is one of the important simulation tools in the study of Electromagnetic propagation. Following the Perfectly Marched Layers (PMLs) proposed by Berenger [8], the absorbing boundary condition was extended to address a wide range of situations. With respect to dispersion which occurs in the FDTD method, there are generally two ways to minimize its effects. The first possibility is to use the Higher Order FDTD technique [9] while the second option is to decrease the size of the unit elements. Here we apply the latter to our problem, i.e., when one twentieth of the signal wavelength (λ) in free space is used as the basic element dimension i.e., the unit cell size, good accuracy can be achieved in a FDTD simulation [10]. We will use this technique to investigate the close to wall antenna radiation pattern (RP) as a function of the distance to the wall (d) and of tunnel walls constructed from materials having different physical constants: relative permittivity (ε_r), relative permeability (μ_r) and conductivity (σ). To simplify the arguments, in our model, we assume that: (a) a point source is deployed on the surface of a flat wall. (b) reflections from other walls are not taken into considerations when conducting our RP calculations.

The paper is organised as the follows. The Two-Element Array Model is briefly introduced in Section 2. The 2D FDTD simulation setup is described in Section 3. In Section 4, the validation of the simulation results is revealed and deployment recommendations are made. Finally, Section 5 draws our conclusions.

2. TWO-ELEMENT ARRAY MODEL

When two identical point sources (S1 and S2) in the horizontal plane synchronously propagate radio waves, a Two-Element Array is formed as shown in Figure 1. Consequently, in the far field (i.e., $r \approx r_1 \approx r_2$

and $\phi \approx \phi_1 \approx \phi_2$), the Array Factor (AF) described in [11, 12] can be expressed as:

$$AF = \cos\left(\frac{\pi D}{\lambda}\cos\phi + \frac{\theta}{2}\right), \quad (1)$$

where ϕ is the azimuth angle, D is the spacing between the two antennas, where $D = 2d$, and θ is the phase difference between the currents driving the antenna elements.

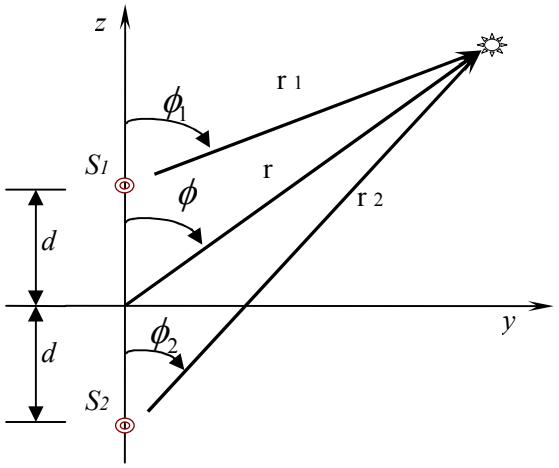

Figure 1: Geometry of the Two-Element Array Model

As we can realise, the AF configuration is equivalent to the scenario when a point source is placed in front of a metal wall (along the direction of y in Figure 1), where ideally the metal acts as a perfect reflector to the point source. In other words, the wave reflected by the wall can be considered as emitted by the image antenna. Therefore in this situation it is appropriate to set $\theta = 180^0$. Although the Two-Element Array Model gives us some basic understanding of the form of the RPs yielded in our investigation, it does not provide us with the additional flexibility to cope with different wall materials, which can be represented as a set of physical constants $(\varepsilon_r, \mu_r, \sigma)$ for each material.

3. FDTD SIMULATION SETUP

As we have found in [13], for a simple structured FDTD model, e.g., the free space model and the plane earth model, we can always use the Modified 2D FDTD simulation instead of a full 3D simulation, provided appropriate correction factors are applied. For the 2D FDTD model in this paper, we use the TM mode, which contains the field components (Ez,Hx,Hy) described in [14]. In the tunnel deployment, this corresponds to positioning a vertical antenna in parallel with and close to the wall and perpendicular to the rails. Within the problem space, we assign the appropriate values of $(\varepsilon_r, \mu_r, \sigma)$ to the corresponding unit cells to represent walls made of cast iron $(\varepsilon_r = 1.0, \mu_r = 1.0, \sigma = 20 \times 10^3)$, concrete $(\varepsilon_r = 7.0, \mu_r = 1.0, \sigma = 0.15)$, which are the main lining materials in tunnels or polythene $(\varepsilon_r = 3.0, \mu_r = 1.0, \sigma = 1.45 \times 10^{-3})$. The remaining unit cells in the problem space are assigned as air $(\varepsilon_r = 1.0, \mu_r = 1.0, \sigma = 0)$. The simulation boundary is terminated by the PMLs. The point source is placed at the positions of interest, i.e., at various spacings from the wall, propagating a sinusoidal signal of frequency 2.40GHz (i.e., λ =12.5cm). After executing the FDTD iterations for a number of time steps until the steady state is reached, signal strength samples are collected. By comparing with the 2D FDTD free space simulation results under the same FDTD parameters, the RP is plotted.

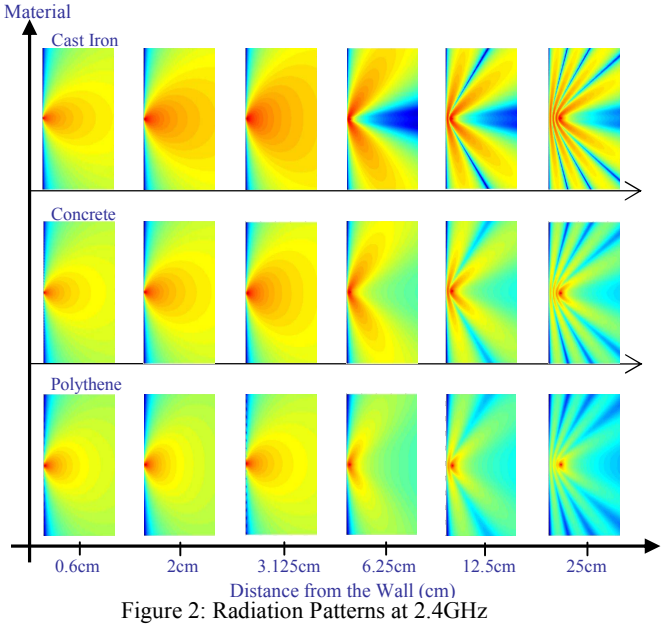

Figure 2: Radiation Patterns at 2.4GHz

4. SIMULATION RESULTS AND ANALYSIS

Owing to the deployment issues, the feasible values of d are less than a few 10s of cm. In our simulations the point source is positioned at 7 different distances away from the wall, specifically 0.6cm $\left(\frac{1}{25}\lambda\right)$, 2cm $\left(\frac{4}{25}\lambda\right)$, 3.125cm $\left(\frac{1}{4}\lambda\right)$, 6.25c $\left(\frac{1}{2}\lambda\right)$, 12.5cm (1λ) and 25cm (2λ).

Figure 2 shows the RPs plotted in the spatial domain (azimuth) for each of the cases described previously, where the dark blue colour represents low radiation gain and the red colour represents high radiation gain. The left boundary of each individual figure has the wall of

different materials terminated. As we can observe from the plots, the RP changes dramatically as the ratio of d to λ is varied. Essentially, we do not want to locate the sensor too close to the wall, since from the 1st column in Figure 2, it can be seen that most of the power is directed toward the opposite wall, which will give poor communication to other sensor nodes mounted along the tunnel. For each of the materials shown in the rows in Figure 2, the RP tends to spread wider and wider as the spacing increases from $\frac{1}{25}\lambda$ up to $\frac{1}{4}\lambda$. However when the distance is further increased, the RP splits initially into two lobes and then more lobes as d is increased further. Between these lobes, we have zones of low gain. Looking at the 4th, 5th, and 6th columns of Figure 2, concrete and polythene walls exhibit less deep nulls than cast iron in the RPs however they have a reduced gain overall owing to energy absorption.

In Figure 3, the RPs are presented in the form of polar plots (in dB). It can be seen that the Two-Element Array solution of Eqn. (1) shows a good fit with the cast iron wall FDTD simulation results while at the same time, the RPs for concrete and polythene walls are also compared. Inside each figure, we define the direction from the center to 0 degree as the normal to the wall and the wall is located in line with -90 degrees and 90 degrees. Based on our findings, when the distance is further away from the wall regardless of its material, the maximum gain is increased. Again we need to ensure that intrusion into the tunnel is minimized while maintaining an acceptable RP. For general wireless communication purposes, at an operating frequency of 2.4GHz, an antenna separation from the wall of at least 2~3cm is recommended.

A tunnel is a special radio propagation environment in the sense that is a largely linear arrangement. In order to maximize the wireless communication range, we in general prefer that the main power lobes point along the tunnel course, which ensures that power is transmitted up and down the tunnel rather than bouncing between walls. We see that this can be achieved by using a spacing of $6.25\text{cm}\left(\frac{1}{2}\lambda\right)$ as shown in the 4th column in Figure 2 or Figure 3(d).

A further preliminary investigation has shown that, by placing a dielectric material in front of cast iron wall, the RP performance can be improved. As an example, we

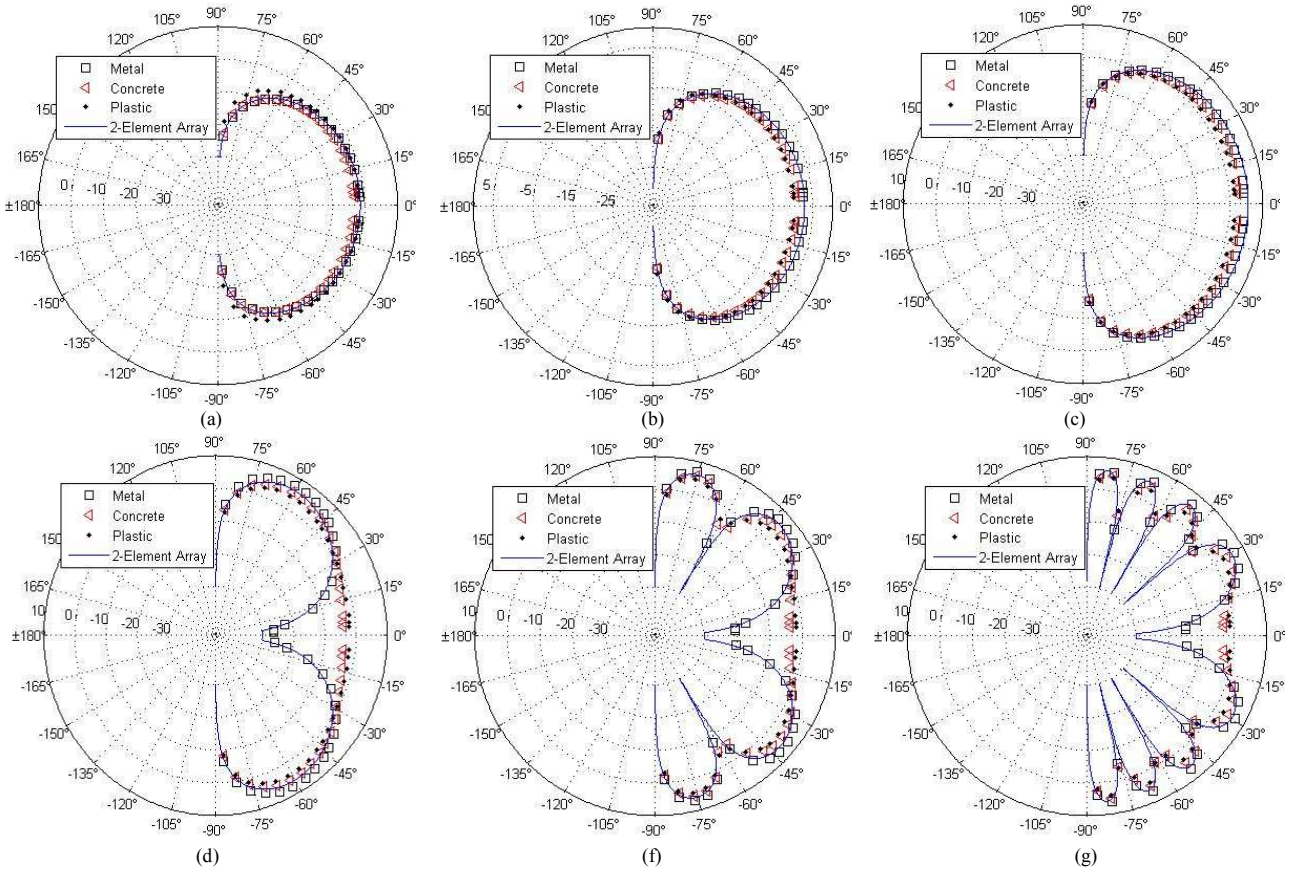

Figure 3. Radiation Patterns at 2.4GHz

added a polythene slab of 6cm in width and 1cm in thickness as illustrated in Figure 4(a). For comparison, we show Figure 4(b) and (c) which corresponding to the 3rd and 4th column of the Cast Iron scenario in Figure 2. As we can observe, Figure 4(d) directs more energy along the tunnel wall than does the arrangement without the dielectric shown in Figure 4(b). Meanwhile it also has a less deep null in the direction (0 degree) normal to the wall and has a smaller spacing from the wall than that of Figure 4(c). Figure 4(e) illustrates the polar plots of the corresponding RPs.

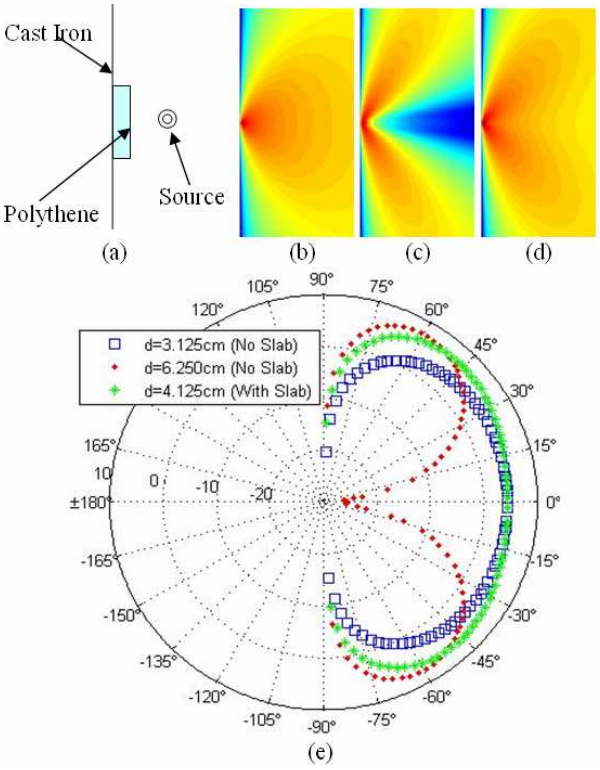

Figure 4: Radiation Pattern Improvement by Adding Dielectric Slab

In practice, the motes operate in the ISM band between 2.405GHz and 2.480GHz. We have also undertaken a set of simulations to determine the stability of the RPs over the specified ISM frequency band. From the results shown in Figure 5, it can be seen that the RPs are reasonably stable, particularly for the practically important close to wall spacings. The largest variation is observed at 0 degrees for the large antenna spacing shown in Figure 5(c).

5. CONCLUSIONS

In this paper, we have discussed the scenario when an antenna is deployed close to a wall. By simply altering the separation distance we have seen that the RPs have dramatically different shapes. Accordingly, we have proposed suitable antenna spacings and a potential design that achieves RPs with suitable directional properties. The construction material affects the overall radiated power since non-metallic materials can absorb significant power.

In order to improve our simulation results from the 2D FDTD method, we can use finer resolution to represent the size of a unit cell, e.g., one fortieth of λ instead of one twentieth of λ. Also according to the definition from the two-element array model, the RPs are calculated via the points of interest in the far field. Here in our simulation model, the RPs are obtained at 20λ distance from the source. Thus we can increase this distance to improve the approximation as indicated in Figure 1. However, both come at the cost of higher computational power in terms of CPU execution time and memory usage.

6. REFERENCES

[1] Y. Wu, M. Lin, and I.J. Wassell, Modified 2D Finite-

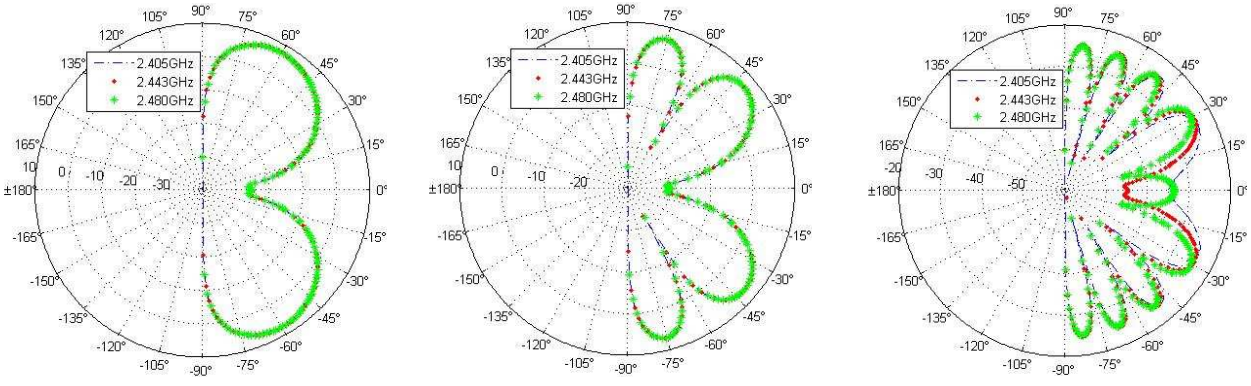

Figure 5: RP Frequency Sensitivity: (a). d = 3.125cm (b). d = 6.25cm (c). d = 25cm

Difference Time-Domain Technique for Tunnel Path Loss Prediction, 2nd International Conference on Wireless Communication in Underground and Confined Areas (To Appear), Aug. 2008.

[2] K.S. Yee, Numerical Solution of Initial Boundary Value Problems involving Maxwell's Equations in Isotropic Media, IEEE Trans. Antennas Propagat., vol. 14, No. 3, pp. 302-307, May 1966.

[3] D. Didascalou, J. Maurer, and W. Wiesbeck, Subway Tunnel Guided Electromagnetic Wave Propagation at Mobile Communications Frequencies, IEEE Trans. Antennas Propagat., vol. 49, No. 11, pp. 1590-1596, Nov. 2001

[4] Y.P. Zhang, Novel Model for Propagation Loss Prediction in Tunnels, IEEE, Trans. Vehicular Technol., vol. 52, No. 5, pp. 1308-1314, Sept. 2003.

[5] C.L. Holloway, D.A. Hill, R.A. Dalke, and G.A. Hufford, Radio Wave Propagation Characteristics in Lossy Circular Waveguides Such as Tunnels, Mine Shafts, and Boreholes, IEEE, Trans. Antennas Propagat., vol. 48, No. 9, pp. 1354-1366, Sept. 2000.

[6] D.G. Dudley, Wireless Propagation in Circular Tunnels, IEEE Trans. Antennas Propagat., vol. 53, No. 1, pp. 435-441, Jan. 2005.

[7] D.J. Cichon, and T. Kurner, *COST Telecommunications – COST Action 231 Digital Mobile Radio Towards Future Generation Systems Final Report*, Chapter 4, Propagation Prediction Models, COST 231 TD(95), pp. 190-195, Sept. 2005.

[8] J.P. Berenger, A Perfectly Matched Layer for the Absorption of Electromagneit Waves, J. Computational Physics, vol. 114, pp. 185-200, 1994.

[9] D. White, M. Stowell, J. Koning, R. Rieben, A. Fisher, N. Madsen, Higher-Order Mixed Finite Element Methods for Time Domain Electromagmetics, UCRL-TR-202339, Internal Report, Feb. 2004.

[10] D.M. Sullivan, Electromagnetic Simulation Using the FDTD Method, Wiley-IEEE Press, pp.8, Jul. 2000.

[11] J. Dunlop and D. G. Smith, Telecommunications Engineering (3rd Edition), Chapman & Hall, 1994.

[12] C.A. Balanis, *Antenna Theory Analysis and Design*, 3rd ed., Chapman & Hall, 2005.

[13] Y. Wu, M. Lin, I.J. Wassell, Path Loss Estimation in 3D Environments using a Modified 2D Finite-Difference Time-Domain Technique, 7th International Conference on Computation in Electromagnetics, Apr. 2008.

[14] A. Taflove and S.C. Hagness, Computational Electrodynamics the Finite-Difference Time-Domain Method, 3rd ed., 2005.